ELSEVIER

Superlattices and Microstructures 33 (2003) 95–101

Superlattices
and Microstructures

www.elsevier.com/locate/jnlabr/yspmi

Raman scattering from three-dimensionally regimented quantum dot superlattices

Olga L. Lazarenkova[a], Alexander A. Balandin[b,*]

[a] *Jet Propulsion Laboratory, California Institute of Technology, 4800 Oak Grove Dr. (MS-169-315), Pasadena, CA 91109-8099, USA*

[b] *Nano-Device Laboratory, Department of Electrical Engineering, University of California—Riverside, Riverside, CA 92521, USA*

Received 17 June 2003; accepted 3 July 2003

Abstract

We examine the low-energy part of Raman scattering spectrum from a three-dimensional regimented array of Ge_xSi_{1-x} quantum dots on Si. Our analysis is based on a numerical solution of the elasticity equation for the whole quantum dot superlattice. Three-dimensional acoustic phonon folding due to structure regimentation and small feature size leads to unique signatures in Raman spectra, which cannot be predicted using the Lamb-type models for quantum dots or the Rytov model for a quantum well superlattice. We found that symmetry breaking, which is achieved when the inter-dot distances are comparable to the dot dimensions, results in increased intensity of confined phonon modes. It is also shown that changes in dot material composition and alteration of the dot size lead to different Raman spectrum modification. The latter can be used as a tool to distinguish phonon confinement effects on Raman spectra from alloying and strain induced effects.

Keywords: Raman spectroscopy; Quantum dot superlattice; Confined phonons; Ge/Si

1. Introduction

Raman spectroscopy has proven to be a powerful tool for investigation of arrays of semiconductor quantum dots [1–3], nanoparticles [4, 5], as well as of nano- and microcrystalline multilayers [6]. It is capable of providing information on modification of vibration spectra of such structures [1, 2] as well as on carrier confinement [3]. Of special interest are phonon confinement effects in quantum dot and nanocrystals [4–9]. They manifest themselves via appearance of additional peaks in the low-frequency

* Corresponding author.
E-mail address: alexb@ee.ucr.edu (A.A. Balandin).

0749-6036/$ - see front matter © 2003 Elsevier Ltd. All rights reserved.
doi:10.1016/S0749-6036(03)00049-1

range [5–7], blue shift of confined acoustic phonon peaks with decreasing nanoparticle size [5–7], as well as red shift and asymmetric broadening of optical phonon peaks [8].

At the same time, interpretation of spectra obtained in Raman scattering experiments with quantum dot samples is plagued with uncertainties and is a subject of continuous debates. It is often difficult to determine whether the change in location and shape of Raman peaks is due to strain, alloying, interdiffusion or it is induced by spatial confinement [9]. When quantum dots form a *regimented* array, the interpretation of Raman spectra becomes an even greater challenge owing to the possible appearance of additional phonon dispersion branches, e.g. standing waves inside or between quantum dots, etc. [10]. This presents a strong motivation for theoretical investigation of Raman spectra of quantum dot arrays.

Most experimental Raman spectra of quantum dots are analyzed [4, 6, 7, 9, 11, 12] on the basis of Lamb's theory [13] or variations thereof, which use vibration modes of a homogeneous elastic body of spherical shape under stress-free boundary conditions. Such analysis does not account for the effect of the surrounding matrix (template, spacers, etc.). In some cases [14] the Raman spectra of quantum dots is interpreted on the basis of the Rytov model [15], which is also a very crude approximation since the Rytov model is essentially one-dimensional and valid for layered media such as quantum well superlattices (QWS). In this paper we present a model based on the exact numerical solution of the elasticity equation for the *whole structure rather than for separate dots*, which allows for accurate interpretation of Raman spectra of three-dimensional (3D) regimented arrays of quantum dots. We argue that it is essential to consider the vibration spectrum of the whole structure in order to obtain correct peak positions and separate the effect of strain or interdiffusion from phonon confinement.

Unlike QWS, the term quantum dot superlattice (QDS), which indicates a multiple array of quantum dots, is conventionally used for structures with or without long-range ordering in the quantum dot position [16]. Partially regimented QDS have been fabricated by a variety of techniques [1, 2, 9, 16]. Nearly perfect two-dimensional (2D) [3] and 3D regimentation have also been achieved [17]. Regimentation along all three directions in such a structure brings an analogy with bulk crystals. In these artificial crystals the role of atoms is played by quantum dots. When the size of the dots is much smaller than the mean-free path (MFP) of acoustic phonons such structure is characterized by its own phonon spectrum and not by the spectrum of individual quantum dots. Here for simplicity we consider an orthorhombic QDS with rectangular parallelepiped shape of the dots. We have previously shown [10] that the carrier and phonon spectrum of QDS is more sensitive to the dot size and regimentation rather than to exact shape. The dot size is chosen to be in the range of 3–9 nm so that it is much smaller than the phonon MFP and laser wavelength ($\lambda = 514$ nm) yet it is large enough for application of the elastic continuum approximation [10].

2. Model

We restrict our analysis to the low frequency part of the spectrum where we expect the most pronounced effects of confinement and regimentation. First the phonon dispersion is

calculated by solving the elasticity equation derived from Euler–Lagrange equations [18] for a non-uniform medium with cubic crystal lattice (see [10] for the details). After phonon dispersion is found we obtain Raman intensities using a macroscopic theory for calculating the photoelasticity tensor [19]. It describes the phonon–photon interaction in the following way. A periodic displacement of geometrical points of the matter $\mathbf{U}(\mathbf{r}, \mathbf{q}, \Omega) = \mathbf{u}(\mathbf{r}, \mathbf{q}, \Omega)\exp(-i\Omega t)$ causes the periodic change of the local strain σ_{ij} which, in turn, locally modulates the dielectric susceptibility $\varepsilon_{ij} = \varepsilon^0_{ij} + \Sigma q_{ijkl}\sigma_{kl}$ of the matter. Here Ω is the phonon frequency, $\mathbf{q}$ is the phonon wavevector, ε^0 is an unperturbed susceptibility tensor, which is diagonal in the main coordinate system of cubic semiconductors, q_{ijkl} are components of the photoelastic tensor. In semiconductors of cubical symmetry there are only two independent non-vanishing components of the photoelasticity tensor q_{1111} and q_{1122}. Thus ε_{ij} perturbed by phonons has only its diagonal components

$$\varepsilon_{xx} = \varepsilon^0_{xx} + q_{1111}\frac{\partial U_x}{\partial x} + q_{1122}\frac{\partial U_y}{\partial y} + q_{1122}\frac{\partial U_z}{\partial z}, \tag{1}$$

with similar expressions for ε_{yy} and ε_{zz} obtained by cyclic exchange of x, y, and z.

An electromagnetic wave with frequency ω and wavevector $\mathbf{k}$ in optically isotropic medium can be characterized by $\mathbf{D} = \hat{\varepsilon}\varepsilon_0\mathbf{A}\exp(i\mathbf{k}\cdot\mathbf{r})\exp(-i\omega t)$. Here ε_0 is the dielectric susceptibility of a vacuum, $\mathbf{A}$ is the light polarization vector, which is perpendicular to the direction of the wave propagation, $|\mathbf{k}| = 2\pi\varepsilon^{1/2}/\lambda$, and λ is the light wavelength in a vacuum. The probability of the scattering process from state $|\mathbf{D}_i\rangle$ to $|\mathbf{D}_f\rangle$ is proportional to the square of the projection of the initial state onto the final one. Since all the eigenstates are orthogonal, the allowed processes are either from the state perturbed by phonon vibration to the unperturbed state, or vice versa. The first process corresponds to light scattering with phonon absorption leading to an anti-Stokes peak shift and the second one corresponds to phonon emission, i.e. Stokes shift. Multi-phonon processes are also allowed but with much less intensity.

Here we limit consideration to one-phonon anti-Stokes processes. The intensity of Stokes peaks in experimental spectra can be found by scaling with the Boltzmann factor [18]. The probability of the scattering process from state $|\mathbf{D}_i\rangle$ to $|\mathbf{D}_f\rangle$ is found as $P_{fi} \propto |\langle\mathbf{D}_f \mid \mathbf{D}_i\rangle|^2$. Substituting an expression for $\mathbf{D}$, taking into account that $|\mathbf{D}_i\rangle$ corresponds to an electromagnetic wave in QDS with dielectric susceptibility (Eq. (1)) perturbed by phonons and applying quasi-periodic boundary conditions, we find the final equation

$$\begin{aligned} P_{fi} \propto (\varepsilon^0)^2\varepsilon_0^4\delta(\omega_f - \omega_i - \Omega)\delta(\mathbf{k}_f - \mathbf{k}_i - \mathbf{q})\left(\frac{V}{d_x d_y d_z}\right)^2\Bigg|_{EC}\int \mathrm{d}\mathbf{r} \\ \times\Bigg\{\exp(-i\mathbf{q}\cdot\mathbf{r})\Bigg[(q_{1111}A_x^iA_x^f + q_{1122}(A_y^iA_y^f + A_z^iA_z^f))\frac{\partial u_x}{\partial x} \\ + (q_{1111}A_y^iA_y^f + q_{1122}(A_z^iA_z^f + A_x^iA_x^f))\frac{\partial u_y}{\partial y} \\ + (q_{1111}A_z^iA_z^f + q_{1122}(A_x^iA_x^f + A_y^iA_y^f))\ \frac{\partial u_z}{\partial z}\Bigg]\Bigg\}\Bigg|^2. \end{aligned} \tag{2}$$

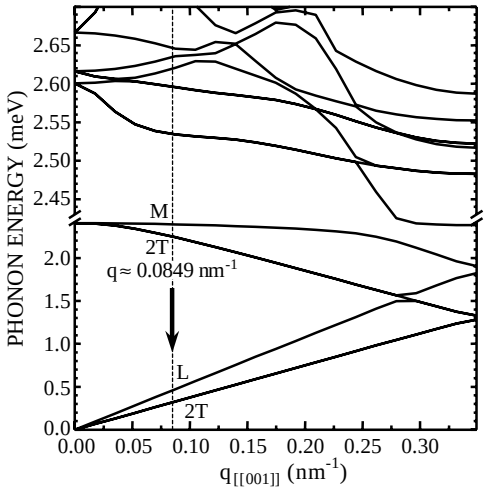

Fig. 1. Lowest phonon dispersion branches in cubic Ge/Si QDS with $L_x = L_y = L_z = 3.0$ nm; $D_x = D_y = D_z = 9.0$ nm. Arrow indicates the wavevector of phonons taking part in Raman back scattering when the normally incident light propagates along [[001]] direction. Note that the magnitude of this wavevector is comparable to the QBZ size.

Eq. (2) in an effective optical medium approximation can be expressed using conventional Raman tensor $\mathfrak{R}$ notation for the *whole* 3D QDS structure via the expression $P_{fi} \propto |\mathbf{A}^f \cdot \mathfrak{R} \cdot \mathbf{A}^i|^2$, where $\mathfrak{R}$ components are determined by an integration of the perturbed dielectric function over the QDS unit cell.

3. Results and discussion

We carry out numerical simulation for GeSi quantum dots on Si with the material parameters taken as in [20]. Fig. 1 shows phonon dispersion for cubical QDS with the dot size of $L = 3.0$ nm and the period of $D = 9.0$ nm. It is usually assumed that in normal-incidence back-scattering configuration the Raman spectroscopy probes the zone-center phonons since transfer momentum is very small compared with the Brillouin zone size, e.g. the wavelength of light is several orders of magnitude larger than the lattice constant. The specific of Raman spectroscopy of regimented arrays of quantum dots is that the momentum $|\mathbf{q}| \cong 2|\mathbf{k}_i|$ is comparable with the size of the quasi-Brillouin zone (QBZ) as indicated by the arrow in Fig. 1. Thus, it is important to know the phonon dispersion accurately when analyzing Raman spectra of QDS. In this figure, the double degenerate transverse mode is marked by $2T$, while longitudinal and mixed modes are marked as L and M, correspondingly. Note, that each phonon branch changes the symmetry of the corresponding vibration in the regions of QBZ where it interacts with other branches.

In Fig. 2(a) we present the calculated Raman spectrum of cubical Ge_xSi_{1-x}/Si QDS for different atomic fraction x of Ge in Ge_xSi_{1-x} quantum dots. In this calculation

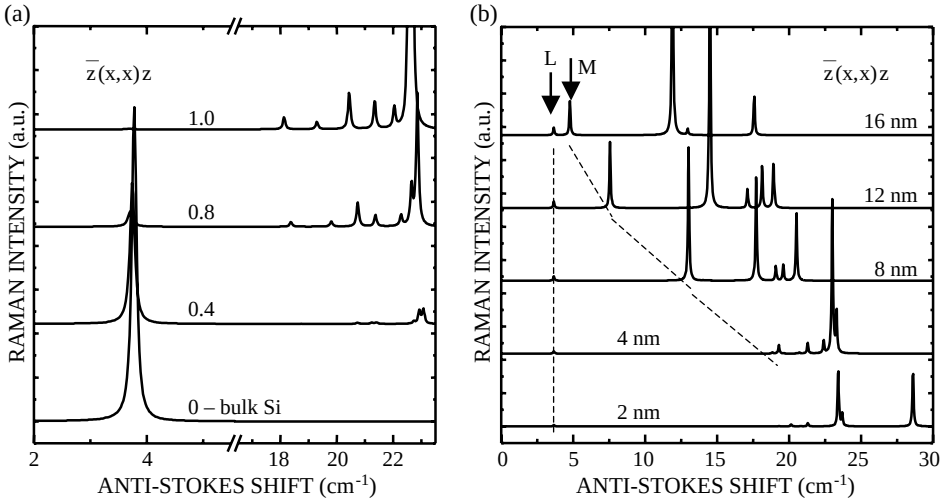

Fig. 2. Raman spectrum of (a) Ge_xSi_{1-x}/Si cubic QDS with fixed dot size of $L_x = L_y = L_z = 3.0$ nm, period $D_x = D_y = D_z = 9.0$ nm and different Ge atomic fraction x; (b) Ge/Si tetragonal QDS with fixed dot base $L_x = L_y = 3.0$ nm and $D_x = D_y = 9.0$ nm, and different $D_z = 2L_z$ along the [[001]] direction of light propagation. To lead the eye the position of the lowest L and M modes is traced with dashed line. Note that due to the change of the symmetry of the QDS unit cell the order of the modes may change.

we assumed that the change in atomic fraction x leads to a linear change in materials parameters and used homogeneous broadening of 0.05 cm^{-1}. The lowest wavenumber peak seen in Fig. 2(a, b) corresponds to the lowest longitudinal acoustic phonon mode of the bulk material. As expected its position is almost not sensitive either to change in atomic fraction or geometry. In the back scattering geometry with the normal incidence of light parallel to the [001] direction of the host cubic semiconductors, the phonon modes are Raman active if they have a longitudinal component of vibrations. Indeed, transverse modes only produce shear vibrations with $du_x/dx = du_y/dy = du_z/dz = 0$ which do not contribute to P_{fi} (see Eq. (2)). The change in Ge atomic fraction leads to two noticeable effects: the shift of Raman peaks and redistribution of their intensity, e.g. gradual damping of the signal from the third branch and increase of the signal from the upper longitudinal and mixed modes. The latter can be traced back to the symmetry breaking of the displacement. Since alloying between Ge dots and Si barrier layers may lead to emergence of extra Si–Ge modes, which are difficult to separate from confined acoustic Ge modes, our results may shed new light on experimental data interpretation [9].

A change in the inter-dot distance between Ge dots in a Si matrix causes nonlinear redistribution of intensities. In two limiting cases of infinitely small and infinitely large inter-dot distances QDS evolves to bulk Ge or Si, respectively. Correspondingly, only the lowest longitudinal mode is active. The upper longitudinal and mixed modes are most intensive when the symmetry breaking is highest. It is achieved when the dot size L is comparable with the inter-dot distance H. The shrinking of the QBZ with increasing $D = H + L$ results in the red shift of these peaks since folding of the acoustic phonon

dispersion branches is attained at lower energies. When the symmetry of QDS is preserved the general structure of the Raman spectrum is the same.

Fig. 2(b) illustrates the effect of the dot shape, i.e. the symmetry breaking, on Raman spectra. The presented results are for the dots with constant base ($L_x = L_y = 3.0$ nm; $D_x = D_y = 9.0$ nm) and changing height of the quantum dot along the [[001]] quasi-crystallographic direction. The inter-dot distance is fixed at $H_z = L_z$. One can see significant redistribution of the peak intensity and strong shift of some peaks, which is a combined effect of the QBZ size decrease in the [[001]] quasi-crystallographic direction and strong modification of phonon dispersion with change of the symmetry. The position of each peak can be traced back to the calculated dispersion (see Fig. 1).

One should note here that the peaks in Fig. 2 have a more complicated structure than typical doublets observed in Raman scattering from folded acoustic phonons in QWS. The position of these peaks could not be deduced from Lamb-type models that use eigenmodes of free-standing nanocrystals.

4. Conclusion

Analysis presented in this paper shows that it is essential to consider the vibration spectrum of the whole structure in order to obtain correct peak positions and separate the effect of strain or interdiffusion from phonon confinement. The proposed approach allows for an accurate analysis of experimental Raman spectra of quantum dot arrays. It can be used to account for the effects of dot regimentation, matrix materials and assist in separation of the spatial confinement effects from alloying and interdiffusion.

Acknowledgements

The work in UCR has been supported in part by the NSF Nanoscale Exploratory Research project ECS-0210282 and NSF CAREER Award No. 0093959 to A.A.B. Part of this work was performed while one of the authors (O.L.L.) held a National Research Council Research Associateship Award at Jet Propulsion Laboratory.

References

[1] J.L. Liu, W.G. Wu, A. Balandin, G. Jin, Y.H. Luo, S.G. Thomas, Y. Lu, K.L. Wang, Appl. Phys. Lett. 75 (1999) 1745; J.L. Liu, Y.S. Tang, K.L. Wang, T. Radetic, R. Gronsky, Appl. Phys. Lett. 74 (1999) 1863.
[2] M. Kuball et al., Appl. Phys. Lett. 78 (2001) 987.
[3] A. Balandin, K.L. Wang, N. Kouklin, S. Bandyopadhyay, Appl. Phys. Lett. 76 (2000) 137.
[4] P. Verma, L. Gupta, S.C. Abbi, K.P. Jain, J. Appl. Phys. 88 (2000) 4109.
[5] V.G. Melehin, V.D. Petrikov, Phys. Low-Dim. Struct. 9/10 (1999) 73.
[6] X.L. Wu, G.G. Siu, M.J. Stokes, S. Tong, F. Yan, X.N. Liu, X.M. Bao, S.S. Jiang, X.K. Zhang, D. Feng, Appl. Phys. Lett. 69 (1996) 1855.
[7] M. Fujii, Y. Kanzawa, S. Hayashi, K. Yamamoto, Phys. Rev. B 54 (1996) R8373.
[8] I.H. Campbell, P.M. Fauchet, Solid State Commun. 58 (1986) 739.
[9] J.L. Liu, G. Jin, Y.S. Tang, Y.H. Luo, K.L. Wang, D.P. Yu, Appl. Phys. Lett. 78 (2001) 1162.
[10] O.L. Lazarenkova, A.A. Balandin, Phys. Rev. B 66 (2002) 245319.
[11] V.G. Melehin, V.D. Petrikov, Phys. Low-Dim. Struct. 9/10 (1999) 73.
[12] A. Tanaka, S. Onari, T. Arai, Phys. Rev. B 47 (1993) 1237.

[13] H. Lamb, Proc. London Math. Soc. 13 (1882) 187.
[14] A. Milekhin, N.P. Stepina, A.I. Yakimov, A.I. Nikiforov, S. Schulze, D.R.T. Zahm, Appl. Surface Sci. 175–176 (2001) 629.
[15] S.M. Rytov, Soviet Phys.–JETP 2 (1956) 466.
[16] K.L. Wang, A. Balandin, Quantum dots: properties and applications, in: V. Markel, T.F. George (Eds.), Optics of Nanostructured Materials, Wiley & Sons, New York, 2000, pp. 515–550.
[17] G. Springholz, M. Pinczolits, P. Mayer, V. Holy, G. Bauer, H.H. Kang, L. Salamanca-Riba, Phys. Rev. Lett. 84 (2000) 4669.
[18] L.D. Landau, E.M. Lifshitz, Theoretical Physics: Theory of Elasticity, vol. 7, 3rd ed., Butterworth-Heinemann, 1995.
[19] P.Y. Yu, M. Cardona, Fundamentals of Semiconductors: Physics and Materials Properties, Springer-Verlag, 1999.
[20] O. Madelung, Landolt-Börnstein (Eds), Physics of Group IV Elements and III–V Compounds, New Series, Group III, vol. 17(a), Springer-Verlag, 1982.